doi:10.2533/chimia.2020.142 Chimia 74 (2020) 142–148

UVB-irradiated Laboratory-generated Secondary Organic Aerosol Extracts Have Increased Cloud Condensation Nuclei Abilities: Comparison with Dissolved Organic Matter and Implications for the Photomineralization Mechanism

Nadine Borduas-Dedekind*[ab], Sergey Nizkorodov[c], and Kristopher McNeill[a]

Abstract: During their atmospheric lifetime, organic compounds within aerosols are exposed to sunlight and undergo photochemical processing. This atmospheric aging process changes the ability of organic aerosols to form cloud droplets and consequently impacts aerosol–cloud interactions. We recently reported changes in the cloud forming properties of aerosolized dissolved organic matter (DOM) due to a photomineralization mechanism, transforming high-molecular weight compounds in DOM into organic acids, CO and CO_2. To strengthen the implications of this mechanism to atmospheric aerosols, we now extend our previous dataset and report identical cloud activation experiments with laboratory-generated secondary organic aerosol (SOA) extracts. The SOA was produced from the oxidation of α-pinene and naphthalene, a representative biogenic and anthropogenic source of SOA, respectively. Exposure of aqueous solutions of SOA to UVB irradiation increased the dried organic material's hygroscopicity and thus its ability to form cloud droplets, consistent with our previous observations for DOM. We propose that a photomineralization mechanism is also at play in these SOA extracts. These results help to bridge the gap between DOM and SOA photochemistry by submitting two differently-sourced organic matter materials to identical experimental conditions for optimal comparison.

Keywords: Cloud condensation nuclei · Dissolved organic matter · Photochemistry · Photomineralization · Secondary organic aerosol

Dr. Nadine Borduas-Dedekind is a Swiss National Science Foundation (SNSF) Ambizione Fellow in the Department of Environmental Science Systems at ETH Zurich. She obtained a Bachelor degree and a Master degree in organic chemistry working on Pd-catalysis and total synthesis as well as in pharmaceutical companies. She then completed her PhD as a Vanier Scholar at the University of Toronto in 2015 and worked on the atmospheric fate of organic nitrogen compounds. After working in air quality consulting in South Africa, she moved to Switzerland as an NSERC postdoctoral fellow in 2016 to study organic aerosol photochemistry and aerosol–cloud properties at ETH Zurich. Her current independent research group is funded by the SNSF and is interested in bringing an organic chemistry perspective to atmospheric processes.

1. Introduction

Uncertainties in aerosol–cloud interactions currently limit our ability to accurately predict cloud location, lifetime and optical properties. Some aerosol particles are able to activate cloud droplets by acting as a hydrophilic surface for water to condense on.[1] Particles capable of growing into cloud droplets under supersaturated conditions, that is, at a relative humidity in excess of 100%, are termed cloud condensation nuclei (CCN). Accordingly, research efforts in the field today are directed towards a physicochemical characterization of aerosols involved in cloud formation for better climate predictions.

In this study, we are specifically interested in measuring the activation of cloud droplets by organic matter, an important constituent of aerosol particles capable of acting as CCN.[2] Indeed, organic compounds account for between 20 to 90% of the total mass of the submicron aerosol population.[3,4] Unlike the photochemically stable inorganic particle constituents, organic compounds experience relatively rapid atmospheric aging by processes such as photochemistry, heterogeneous oxidation, gas-particle partitioning and cloud processing.[1,5–8] In particular, exposure to sunlight is an effective atmospheric aging process since photochemistry can lead to direct photolysis of organic compounds and to indirect processes, such as generation of reactive oxygen species and electronically excited-state organics.[5,9,10] These reactive species can subsequently induce further chemical transformations of organic compounds in aerosol particles including oxidation,

*Correspondence: Dr. N. Borduas-Dedekind[ab], E-mail: Nadine.borduas@usys.ethz.ch
[a]Institute for Biogeochemistry and Pollutant Dynamics, ETH Zurich, Universitätstrasse 16, CH-8092 Zurich, Switzerland; [b]Institute for Atmospheric and Climate Sciences, ETH Zurich, Universitatstrasse 16, CH-8092 Zurich, Switzerland, [c]Department of Chemistry, University of California, Irvine, 377 Rowland Hall, Irvine, USA

addition, fragmentation and condensation reactions. Along with the chemical complexity and heterogeneity of organic aerosols, these processes complicate our ability to reliably describe interactions between aerosols, solar radiation and clouds in climate models. In the atmosphere, it is likely that all these aging reactions are occurring simultaneously, but we turn to laboratory studies for controlled experiments to study the effects of photochemistry alone.

This study focuses on quantifying the effect of atmospheric aqueous photochemistry in cloud and fog droplets on the CCN ability of organic matter. Aqueous photochemistry processing of aerosols has been observed in ambient field measurements and is competitive with surface gas-phase oxidation for transforming the photochemical properties of aerosols.[11–14] After a CCN particle grows into a droplet, its water-soluble compounds can engage in aqueous photochemical processes, and once water evaporates, the residual particle will have a different chemical composition. Until recently, it was not known whether cloud-processed organic particles have different CCN activity compared to the particles that activated the droplet in the first place. Towards this goal, we recently reported that photochemical exposure of field-collected dissolved organic matter (DOM) from rivers and swamps in the United States lead to important changes in the DOM's ability to activate cloud droplets and to nucleate ice crystals.[15] Using chemical analyses, we observed that the total content of organic matter decreased during irradiation, with a concurrent production of organic acids, CO and CO_2. These observations support a photomineralization mechanism, wherein direct and indirect photochemical processes lead to the oxidation of the organic material up to the highest form of oxidized carbon, CO_2. We speculated that the conversion of organic matter to CO_2, in other words, the photomineralization mechanism, is responsible for a decrease in the organic-to-inorganic compound ratio within the aqueous aerosol, and thus for an increase in the ability of that particle to grow into a cloud droplet.[15] However, the question remains to be answered whether this mechanism identified in river and swamp DOM samples can be extrapolated to atmospheric organic aerosol samples. We hypothesized that it can be, and here we describe experiments to support this hypothesis.

Thus, this study aims to directly compare the changes in CCN abilities of DOM and of secondary organic aerosol (SOA) extracts under conditions of photomineralization. SOA are formed from the oxidation of volatile organic compounds (VOCs) emitted into the atmosphere. These organic compounds can be of biogenic origin, such as isoprene, monoterpenes and sesquiterpenes, and of anthropogenic origin, such as polycyclic aromatic hydrocarbons. Once in the atmosphere, these VOCs will be oxidized by hydroxyl radicals, ozone, and nitrate radicals. The oxidation products tend to have lower volatility and can nucleate particles after overcoming a critical size for clustering[16] or can partition into pre-existing particles. Here, we generated SOA from the oxidation of a reprsentative biogenic VOC, α-pinene, and of a representative anthropogenic VOC, naphthalene, using an established smog chamber method.[17] Once collected on filters, we extracted the water-soluble organic fraction and submitted the solutions to UVB irradiation equivalent to 4.6 days in the atmosphere at mid-latitudes in summertime. We then re-aerosolized these solutions within an experimental setup equipped with particle sizing and particle counting instrumentation as well as a CCN counter. We find that solutions of both DOM and SOA showed increased hygroscopicity, further quantified with κ values based on Köhler theory, and thus increased CCN ability with photooxidation, consistent with our hypothesis. In all, we seek to show that laboratory-generated SOA extracts compare with DOM in their abilities to act as CCN under photomineralization conditions.

2. Methods

2.1 *SOA Collection*

The α-pinene and naphthalene SOA were generated inside a ~5 m^3 smog chamber made of Teflon according to a previously published method.[17,18] Briefly, α-pinene and naphthalene were injected into the chamber to achieve mixing ratios of 0.50 and 0.40 ppmv (part per million by volume), respectively (Table 1). The α-pinene SOA was produced by the addition of 3.0 ppmv of ozone, whereas the naphthalene SOA was produced by the addition of 2.0 ppmv of hydrogen peroxide and of 0.40 ppmv of nitric oxide followed by exposure to UVB lights (Solar Tec Systems, Inc.) centered at 310 nm. The starting mixing ratios of the VOCs and oxidants were high; they do not accurately represent ambient concentrations of these molecules, but rather they allow for the generation of sufficient SOA mass for subsequent experiments. The reaction time for both SOA types ranged from 1 to 2.3 h and the aerosols produced were collected unto 0.2 μm pore size PTFE filters (FGLP04700 from Millipore) at 15 L min^{-1} for approximately 4 h (Table 1). The filters were then sealed under vacuum, shipped and kept frozen until extraction. The chamber was cleaned with high levels of OH radicals, ozone and high humidity in between samples.

2.2 *SOA Extraction*

The filter samples were kept in a freezer for two months before extraction. The two naphthalene filters were combined to achieve a higher concentration in the extract in pre-washed and pre-baked at 120 °C 100 mL amber Schott glass vials; the same was done for the two α-pinene filters. They were then immersed in MilliQ water and shaken on a shaker for 3 h. The naphthalene SOA solution was yellow and the α-pinene solution was colorless, in agreement with previous observations.[8,19]

2.3 *TOC Analysis*

To measure the organic carbon content, 6.8 mL of each SOA solution was used on a TOC analyzer (Shimadzu, model TOC-L

Table 1. List of experimental parameters for the production and collection of SOA filter samples. All experiments were conducted under dry conditions (0% RH). The SOA-generation method is described in detail in Malecha *et al.*[17] The filter collection time was approximately 4 h for all experiments.

VOC	VOC conc. [ppmv]	Oxidant	Oxidant conc. [ppmv]	UVB light [h]	Reaction time [h]	Max. particle conc. [mg m^{-3}]	SOA mass collected [mg]
naphthalene	0.40	H_2O_2 / NO	2.00 / 0.40	2.25	2.3	876	2.20
naphthalene	0.40	H_2O_2 / NO	2.00 / 0.40	2.25	2.3	700	1.06
α-pinene	0.50	O_3	3.00	dark	1	1840	1.74
α-pinene	0.50	O_3	3.00	dark	1	1950	1.68

CSH) coupled to an autosampler (Shimadzu, model ASI-L). The TOC concentrations reported are measured as the non-purgeable organic carbon mass in mg of carbon per liter (mg C L^{-1}). The α-pinene SOA and the naphthalene SOA solutions contained 13.5 ± 0.1 mg C L^{-1} and 16.4 ± 0.1 mg C L^{-1}, respectively and were used as is for the CCNC experiments.

2.4 *Photochemical Experiments*

The SOA solutions were exposed to identical photochemical experiments as the DOM solutions previously described in Borduas-Dedekind *et al.*[15] The solutions were irradiated in cork-capped 10-mL borosilicate test tubes (Pyrex, 15 × 85 mm, disposable) inside a commercial photochemical Rayonet reactor with six UVB bulbs (3000 Å, Southern New England Ultraviolet Co.). There was enough extracted SOA solution for 9 irradiation time points; at each time point a test tube was removed from the photochemical reactor, transferred to a precleaned amber vial and kept in the fridge at 4 °C until further experiments. The photochemical reactor had a fan to keep the temperature constant at 30–32 °C. Following the actinometry experimental results previously reported for this exact setup,[15] we estimated that 25 h of UVB exposure inside the photochemical reactor is equivalent to 4.6 days in the atmosphere at mid-latitudes in summertime.

2.5 *CCNC Experimental Setup*

The main experimental setup used in this study involved a commercial cloud condensation nuclei counter (CCNC, Droplet Measurement Technologies) and was identical to the setup employed in the measurement of the DOM solutions[15] (Fig. 1). This instrument operates on the principle that water vapor travels faster than heat in air, which consequently creates a constant supersaturation within an air flow in the middle of an insulated column.[20,21] The bottom of the CCNC column is also equipped with an optical particle counter to measure droplet sizes in the range of 0.75 to 10 μm (Fig. 1). Prior to entering the CCNC, the flow of aerosolized SOA was dried by passing through silica gel and 4 Å molecular sieves diffusion dryers and subsequently size-selected by a differential mobility analyser (DMA, TSI Model 3082) and counted by a condensation particle counter (CPC, TSI Model 3772). The flow of monodispersed dried aerosols was then pulled into the CCNC. The calibrated sample and sheath flows were 0.05 and 0.45 L min^{-1} respectively, and the supersaturation and temperature were calibrated using a 5.0 mM solution of $(NH_4)_2SO_4$. The supersaturation value was chosen for optimal measurement of the inflection point of the CCN fraction curve as a function of dry diameter (Fig. 2). The CCN fraction of the aerosolized SOA solution was determined by scanning the aerodynamic diameter on the DMA at intervals of a minimum of 2 min while the CCNC was set to a fixed supersaturation either at 0.30% or at 0.40% above 100% RH (Fig. 2).

The data analysis for the CCN measurements involved importing the CCNC data, the CPC data and the diameter information which was recorded during the experiment into a data-analysis and visualization software (IGOR Pro, Wavemetrics). All measurements were time-matched and the CCN fraction time series was generated by dividing the CCNC data by the CPC data. Then, for each diameter, the CCN fraction was calculated and plotted vs. dry aerodynamic diameter for a specific supersaturation condition (Fig. 2). A sigmoidal fit was obtained from these curves normalized to unity[20,22] and used to determine the critical diameter, that is, the diameter at which the CCN fraction is equal to 50% of the aerosols activated as cloud droplets (Table 2). Doubly charged particles originating from the DMA size selection were evident in the CCN fraction curves, but contributed only to approximately 10% of the CCN activation. Correcting for the doubly charged particles led to a difference of up to 1% in critical diameter calculations consistent with Paramonov *et al.*,[22] and therefore we did not correct further. To calculate the hygroscopicity parameter κ, the simplified equation, Eqn. (1), from Petters and Kreidenweis,[23] was used:

$$\kappa = \frac{4}{27 D_d^3 (\ln S_c)^2} \left(\frac{4\sigma_{s/a} M_w}{RT\rho_w} \right)^3 \quad (1)$$

where S_c is the supercritical saturation at which the CCNC was operated, D_d is the dry diameter (in m, measured by the DMA), κ is the hygroscopicity parameter (unitless), $\sigma_{s/a}$ is the surface tension of water (0.072 J m^{-2}), M_w is the molecular weight of water (18 g mol^{-1}), R is the universal gas constant (8.314 J K^{-1} mol^{-1}), T is the temperature of the inlet flow (298 K) and ρ_w is the density of water (10^6 g m^{-3}).[23] This equation can be used here as κ values were close to or greater than the 0.2 threshold.[23] Furthermore, to ensure that none of the evaluated chemistry came from the filters, we verified that blank filter extracts did not generate any aerosols, and consequently no CCN. Water blanks through the setup in Fig. 1 led to zero CCN counts, but did generate tens of particles per cubic centimeter of aerodynamic diameters below 40 nm, and were thus considered negligible during experiments of particle counts between 1000 and

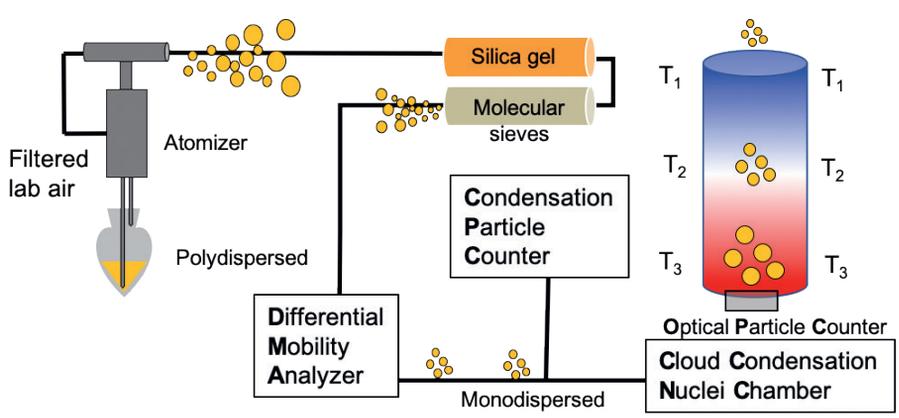

Fig. 1. Experimental setup used to measure the cloud condensation nuclei (CCN) ability of aqueous solutions of organic matter. The aqueous solution was first aerosolized and then dried through silica gel and molecular sieves, thereby decreasing the size of the polydispersed flow of aerosols from the atomizer. The dry polydispersed aerosol flow was then size-selected by a differential mobility analyzer (DMA) to produce a monodispersed aerosol flow and was subsequently counted by an optical particle counter within a commercial cloud condensation nuclei counter (CCNC). There are three temperature controls along the CCNC column (T1, T2, and T3) which range from cold to warm and which are adjusted to generate different super saturation conditions.

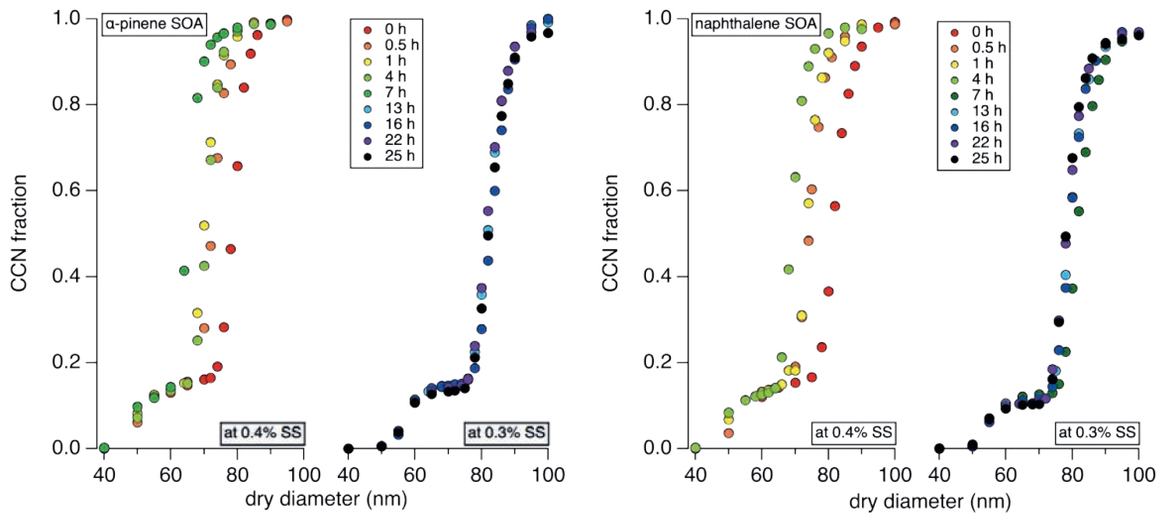

Fig. 2. CCN fraction curves as a function of dry diameter for α-pinene SOA (left panel) and for naphthalene SOA (right panel) for the determination of the critical diameter at 50% activation. A total of 9 curves was measured between 0 h and 25 h of UVB exposure equivalent to approximately 4.6 days in the atmosphere at supersaturations of 0.4% and 0.3% for the least and most hygroscopic samples, respectively. Different supersaturation conditions enabled the optimal measurement of the inflection point of the curve fitted using a sigmoidal curve. The pedestals in the curves correspond to the activation of larger doubly charged particles passing through the DMA, but since corrections for the doubly charged particles led to differences of up to 1% in the critical diameter, no corrections were made for the calculation of κ values.

Table 2. CCN data obtained from the CCN fraction curves in Fig. 2 and measured from the CCNC setup depicted in Fig. 1. SS% is defined as the supersaturation above 100% and the critical diameter is the value at 50% activated CCN fraction.

Hours of UVB exposure	α-Pinene SOA			Naphthalene SOA		
	SS%	Critical diameter [nm]	κ value	SS%	Critical diameter [nm]	κ value
0	0.28	78.3	0.18	0.28	81.3	0.16
0.5	0.40	72.2	0.23	0.40	74.0	0.21
1	0.40	69.7	0.25	0.40	73.4	0.22
4	0.40	70.4	0.24	0.40	68.7	0.26
7	0.40	64.6	0.31	0.30	81.4	0.28
13	0.30	81.7	0.28	0.30	78.9	0.31
16	0.30	82.8	0.27	0.30	79.1	0.31
22	0.30	81.3	0.28	0.30	78.2	0.32
25	0.30	81.9	0.28	0.30	78.0	0.32

3000 cm^{-3}. Finally, the instrumental uncertainty in κ was ± 0.01, obtained as the standard error of triplicate measurements, and the plotted κ values in Fig. 3 represent the range of values from repeated measurements. We had limited amounts of SOA extracts and so could not repeat the experiments as many times as with the DOM solutions.

3. Results and Discussions

3.1 *TOC of SOA*

We first determined the TOC content of α-pinene and naphthalene SOA extract solutions to be 13.5 ± 0.1 mg C L^{-1} and 16.4 ± 0.1 mg C L^{-1}, respectively. This mass was extracted from the SOA filters using only water, and therefore should be considered as the water-soluble organic fraction. Based on previous measurements, more than 80% of the α-pinene and naphthalene SOA material is expected to be extractable in water.[19] The TOC concentrations are relevant to organic matter concentrations found in cloud water; for example, Cook *et al.* measured a range of organic matter in cloud water of 0.73–16.6 mg C L^{-1}.[24] These concentrations are also within the range of TOC from the solutions of DOM in this comparison study, specifically 14–21 mg C L^{-1},[15] establishing that the TOC in both the SOA and DOM were comparable for the CCNC experiments.

3.2 *CCN Ability of Irradiated SOA*

Next, the CCN fraction curves of the SOA extracts were measured as a function of dry diameter at a set supersaturation within the experimental setup depicted in Fig. 1. A total of nine SOA solutions from both α-pinene and naphthalene SOA were exposed to UVB irradiation for up to 25 h and measured on the CCNC (Table 2). The obtained CCN fraction curves showed a translation towards smaller dry diameters as a function of photooxidation up until 4 to 7 h of UVB irradiation (Fig. 2). This decrease in critical diameter represents an increase in CCN ability, further quantified by increasing κ values, calculated using Eqn. (1) (Table 2). Indeed, the κ values for irradiated α-pinene and naphthalene SOA extracts increased from 0.17 to 0.28 and from 0.16 to 0.32, respectively. Most of the increase in kappa values took place within 1 h of photochemical processing, perhaps connected to a burst of OH radical production recently observed due to peroxides albeit

with iron.[25] Prolonged irradiation of the samples up to 25 h in our photoreactor did not lead to further significant increases in CCN abilities (Table 2). Nonetheless, the κ values increased by a factor of 2 for naphthalene SOA over 25 h of UVB irradiation or 4.6 days of equivalent sunlight.

The CCN measurements of the SOA extracts compare well with field measurements. Indeed, in Hyytiälä, Finland, where the majority of the organic aerosol mass is from biogenic SOA, average κ values obtained with comparable experimental and data processing techniques at 0.40 SS%, that is supersaturation conditions above 100%, were ~0.13.[22] Our laboratory-generated α-pinene SOA sample had a κ value of 0.18 before any photooxidation (Table 2). Furthermore, the CCN abilities of the SOA extracts reported in this study fall within the global average estimate of κ values of ~0.3 based on a harmonized CCN worldwide dataset.[26] In addition, a summary of CCN abilities of ambient aerosols across different field campaigns and monitoring stations determined that the CCN activated fraction (AF) of an aerosol population can be fitted by the expression AF = 0.22 ln (SS%) + 0.69.[27] Using Eqn. (1), we can calculate that an increase in κ values due to photochemistry from 0.18 to 0.28, such as measured in this study for α-pinene SOA, for a particle of dry dimeter equal to 80 nm leads to a decrease in required supersaturation from 0.38% to 0.31%. This change in supersaturation, according to the overall fitted data in Paramonov *et al.*,[27] can be equated to an increase in AF of 0.05. Although we show that photochemical exposure equivalent to 4.6 days in the atmosphere increases the CCN abilities of α-pinene and naphthalene SOA solutions, the increase is arguably negligible within the variability of recent worldwide CCN datasets.[2,26,27]

3.3 *Comparison of CCN ability of SOA and of DOM*

To help bridge the gap between DOM and SOA photochemistry, we compare the CCN abilities of previously reported field-collected and purchased DOM samples[15] with the laboratory-generated α-pinene and naphthalene SOA reported here. We make this comparison by plotting the hygroscopicity κ values for both α-pinene and naphthalene SOA as well as for DOM as a function of UVB exposure under identical reaction conditions (Fig. 3). Indeed, the increase in κ values with irradiation is consistent across all tested samples, including field-collected DOM from the Great Dismal Swamp in Virginia in 2014 and in 2016 and from the Suwannee River in Florida in 2017 as well as purchased DOM standard of Suwannee River fulvic acid and finally α-pinene and naphthalene SOA. The similarity in the CCN ability increasing trend of organic matter from rivers and from the atmospheric proxies supports the view that the photomineralization mechanism identified in DOM samples is also at play in the SOA solution samples.

There continues to be discussion concerning the similarities and differences between aquatic and atmospheric organic matter.[28] Similarities between DOM and SOA can be made concerning a subset of aerosols, for example lake-spray aerosols, which are organic aerosols generated directly from aquatic DOM.[29] There also exist complex organic molecules, including humic-like substances within atmospheric aerosols.[30,31] An important difference between the DOM and the SOA samples discussed within this study are their formation mechanism. The SOA reported here were generated in a controlled smog chamber oxidation experiment by oxidation of a single VOC. These laboratory-generated SOA samples certainly have a lower diversity of chemical compounds, including chromophores than the DOM samples in this comparison. Yet, a similar increase in the CCN efficiency compared to more chemically complex DOM samples was observed.

Furthermore, during photochemistry, many reactive intermediates can be produced including OH radicals, peroxides, singlet oxygen and triplet state organic matter. We recently investigated the ability of the identical SOA extracts reported in this study to sensitize singlet oxygen.[18] We found that although naphthalene SOA could effectively sensitize singlet oxygen at comparable efficiencies to DOM, α-pinene SOA extracts were unable to sensitize singlet oxygen within the detection limits of our furfuryl alcohol probe technique.[18] Although we can argue that singlet oxygen played a negligible role in the photomineralization of the α-pinene SOA extracts, OH radicals and organic peroxides likely

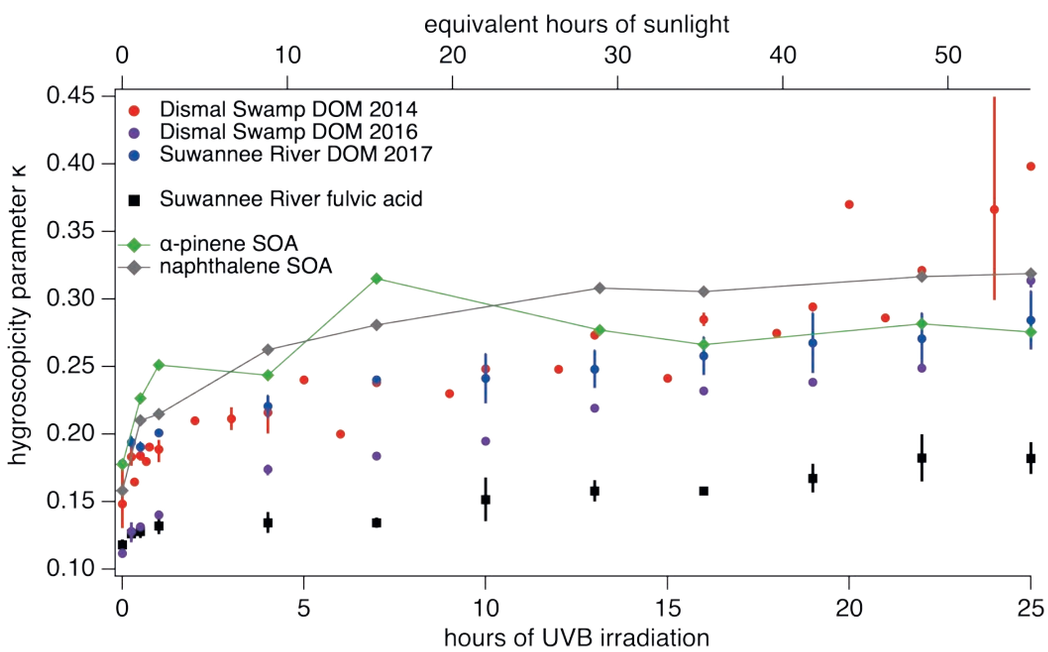

Fig. 3. The CCN ability of α-pinene and naphthalene SOA increases as a function of irradiation similarly to field-collected DOM and to Suwannee River fulvic acid (SRFA) from Borduas-Dedekind *et al.*[15] The experimental conditions are equivalent to up to 25 h of UVB exposure (~55 h or 4.6 days of sunlight at mid-latitudes in summer in the atmosphere). The colors indicate different source material (DS 2014 in red, DS 2016 in purple, SR 2017 in blue, SRFA in black, α-pinene SOA in green and naphthalene SOA in grey), and the symbols indicate that the material was field-collected (circles), commercially available (squares) or lab-generated (diamonds). The instrumental uncertainty in κ is ± 0.01, corresponding to a standard error of triplicate measurements. To show the spread of the measurements, the range from multiple photochemical experiments representing reproducibility are illustrated as bars. For the SOA samples, the markers are connected with a line for visual enhancement.

were also generated in both SOA samples, contributing to an increase in oxidized carbon, concurrent with the fragmentation of molecules yielding small molecules including CO and CO_2.

4. Conclusions and Outlook

The goal of this study was to compare the CCN ability of laboratory-generated biogenic and anthropogenic SOA to aquatic DOM under UVB irradiation. We had previously observed an increasing CCN ability of photooxidized DOM consistent with a photomineralization mechanism. However, since the organic matter in the field-collected DOM samples originated from aquatic environments, the atmospheric relevance of the photomineralization mechanism remained unclear. Here, we demonstrate that SOA made from ozonolysis of α-pinene and from OH radical oxidation of naphthalene also demonstrated increasing CCN ability with aqueous photooxidation. CCN measurements were used to calculate hygroscopicity κ values, and we monitored how this value increased with UVB exposure time.[15] Indeed, both SOA types showed increases in κ values and thus in CCN ability with photooxidation equivalent to 4.6 days in the atmosphere. The main conclusion of this study is that solutions of DOM and SOA, requiring a supersaturation to initially activate cloud droplets, will become better CCN after photochemical cloud-processing, and will be able to re-activate cloud droplets at lower supersaturations. Indeed, we measured κ values increasing from 0.16 to 0.32 for SOA and from 0.12 to 0.40 for DOM. The caveat of our work lies in the extension of aqueous phase photochemistry to particle-phase photochemistry, which cannot be reconciled with our experimental setup. This study further helps extend the photomineralization mechanism to atmospherically relevant atmospheric aqueous aerosols. Our research contributes to the field of atmospheric science by highlighting the importance and complexity of the role of chemistry in aerosol–cloud interactions. As these interactions are critical parameters in predicting future climate forcing, understanding the role of changing aerosol chemistry for particles acting as CCN can help build more accurate parameterizations.

Acknowledgements

The authors acknowledge the technical help of graduate student Kurtis Malecha with the SOA collection. The authors are also grateful to Dr. Zamin Kanji and Prof. Dr. Ulrike Lohmann for the use of the cloud condensation nuclei counter in their laboratory at ETH Zurich.

Financial support

N.B.D acknowledges support from the SNSF Ambizione fellowship (grant no PZ00P2_179703). S.N. acknowledges support from US NSF (grant AGS-1853639).

Received: December 25, 2019

[1] D. K. Farmer, C. D. Cappa, S. M. Kreidenweis, *Chem. Rev.* **2015**, *115*, 4199, DOI: 10.1021/cr5006292.

[2] J. Schmale, S. Henning, S. Decesari, B. Henzing, H. Keskinen, K. Sellegri, J. Ovadnevaite, M. Pöhlker, J. Brito, A. Bougiatioti, A. Kristensson, N. Kalivitis, I. Stavroulas, S. Carbone, A. Jefferson, M. Park, P. Schlag, Y. Iwamoto, P. Aalto, M. Äijälä, N. Bukowiecki, M. Ehn, R. Fröhlich, A. Frumau, E. Herrmann, H. Herrmann, R. Holzinger, G. Kos, M. Kulmala, N. Mihalopoulos, A. Nenes, C. O'Dowd, T. Petäjä, D. Picard, C. Pöhlker, U. Pöschl, L. Poulain, E. Swietlicki, M. Andreae, P. Artaxo, A. Wiedensohler, J. Ogren, A. Matsuki, S. Soo Yum, F. Stratmann, U. Baltensperger, M. Gysel, *Atmos. Chem. Phys.* **2018**, *18*, 2853, DOI: 10.5194/acp-18-2853-2018.

[3] J. L. Jimenez, M. R. Canagaratna, N. M. Donahue, A. S. H. Prevot, Q. Zhang, J. H. Kroll, P. F. DeCarlo, J. D. Allan, H. Coe, N. L. Ng, A. C. Aiken, K. S. Docherty, I. M. Ulbrich, A. P. Grieshop, A. L. Robinson, J. Duplissy, J. D. Smith, K. R. Wilson, V. A. Lanz, C. Hueglin, Y. L. Sun, J. Tian, A. Laaksonen, T. Raatikainen, J. Rautiainen, P. Vaattovaara, M. Ehn, M. Kulmala, J. M. Tomlinson, D. R. Collins, M. J. Cubison, E. J. Dunlea, J. A. Huffman, T. B. Onasch, M. R. Alfarra, P. I. Williams, K. Bower, Y. Kondo, J. Schneider, F. Drewnick, S. Borrmann, S. Weimer, K. Demerjian, D. Salcedo, L. Cottrell, R. Griffin, A. Takami, T. Miyoshi, S. Hatakeyama, A. Shimono, J. Y. Sun, Y. M. Zhang, K. Dzepina, J. R. Kimmel, D. Sueper, J. T. Jayne, S. C. Herndon, A. M. Trimborn, L. R. Williams, E. C. Wood, A. M. Middlebrook, C. E. Kolb, U. Baltensperger, D. R. Worsnop, *Science* **2009**, *326*, 1525, DOI: 10.1126/science.1180353.

[4] Y. Zhang, H. Forrister, J. Liu, J. Dibb, B. Anderson, J. P. Schwarz, A. E. Perring, J. L. Jimenez, P. Campuzano-Jost, Y. Wang, A. Nenes, R. J. Weber, *Nature Geosci.* **2017**, *10*, 486, DOI: 10.1038/ngeo2960.

[5] C. George, M. Ammann, B. D'Anna, D. J. Donaldson, S. A. Nizkorodov, *Chem. Rev.* **2015**, *115*, 4218, DOI: 10.1021/cr500648z.

[6] A. Laskin, J. Laskin, S. A. Nizkorodov, *Chem. Rev.* **2015**, *115*, 4335, DOI: 10.1021/cr5006167.

[7] B. Ervens, *Chem. Rev.* **2015**, *115*, 4157, DOI: 10.1021/cr5005887.

[8] D. E. Romonosky, N. N. Ali, M. N. Saiduddin, M. Wu, H. J. (Julie) Lee, P. K. Aiona, S. A. Nizkorodov, *Atmos. Environ.* **2016**, *130*, 172, DOI: 10.1016/j.atmosenv.2015.10.019.

[9] K. McNeill, S. Canonica, *Environ. Sci.: Processes Impacts* **2016**, *18*, 1381, DOI: 10.1039/C6EM00408C.

[10] H. Chen, X. Ge, Z. Ye, *Curr. Pollution Rep*. **2018**, *4*, 8, DOI: 10.1007/s40726-018-0079-7.

[11] X. Ge, Q. Zhang, Y. Sun, C. R. Ruehl, A. Setyan, *Environ. Chem.* **2012**, *9*, 221, DOI: 10.1071/EN11168.

[12] S. Gilardoni, P. Massoli, M. Paglione, L. Giulianelli, C. Carbone, M. Rinaldi, S. Decesari, S. Sandrini, F. Costabile, G. P. Gobbi, M. C. Pietrogrande, M. Visentin, F. Scotto, S. Fuzzi, M. C. Facchini, *Proc. Natl. Acad. Sci. U.S.A.* **2016**, *113*, 10013, DOI: 10.1073/pnas.1602212113.

[13] W. Xu, T. Han, W. Du, Q. Wang, C. Chen, J. Zhao, Y. Zhang, J. Li, P. Fu, Z. Wang, D. R. Worsnop, Y. Sun, *Environ. Sci. Technol*. **2017**, *51*, 762, DOI: 10.1021/acs.est.6b04498.

[14] S. Dasari, A. Andersson, S. Bikkina, H. Holmstrand, K. Budhavant, S. Satheesh, E. Asmi, J. Kesti, J. Backman, A. Salam, D. S. Bisht, S. Tiwari, Z. Hameed, Ö. Gustafsson, *Sci. Adv.* **2019**, *5*, eaau8066, DOI: 10.1126/sciadv.aau8066.

[15] N. Borduas-Dedekind, R. Ossola, R. O. David, L. S. Boynton, V. Weichlinger, Z. A. Kanji, K. McNeill, *Atmos. Chem. Phys.* **2019**, *19*, 12397, DOI: https://doi.org/10.5194/acp-19-12397-2019.

[16] M. Kulmala, J. Kontkanen, H. Junninen, K. Lehtipalo, H. E. Manninen, T. Nieminen, T. Petäjä, M. Sipilä, S. Schobesberger, P. Rantala, A. Franchin, T. Jokinen, E. Järvinen, M. Äijälä, J. Kangasluoma, J. Hakala, P. P. Aalto, P. Paasonen, J. Mikkilä, J. Vanhanen, J. Aalto, H. Hakola, U. Makkonen, T. Ruuskanen, R. L. Mauldin III, J. Duplissy, H. Vehkamäki, J. Bäck, A. Kortelainen, I. Riipinen, T. Kurtén, M. V. Johnston, J. N. Smith, M. Ehn, T. F. Mentel, K. E. J. Lehtinen, A. Laaksonen, V.-M. Kerminen, D. R. Worsnop, *Science* **2013**, *339*, 943, DOI: 10.1126/science.1227385.

[17] K. T. Malecha, S. A. Nizkorodov, *Environ. Sci. Technol.* **2016**, *50*, 9990, DOI: 10.1021/acs.est.6b02313.

[18] A. Manfrin, S. A. Nizkorodov, K. T. Malecha, G. J. Getzinger, K. McNeill, N. Borduas-Dedekind, *Environ. Sci. Technol*. **2019**, *53*, 8553, DOI: 10.1021/acs.est.9b01609.

[19] H. J. Lee, P. K. Aiona, A. Laskin, J. Laskin, S. A. Nizkorodov, *Environ. Sci. Technol.* **2014**, *48*, 10217, DOI: 10.1021/es502515r.

[20] D. Rose, S. S. Gunthe, E. Mikhailov, G. P. Frank, U. Dusek, M. O. Andreae, U. Pöschl, *Atmos. Chem. Phys.* **2008**, *8*, 1153, DOI: 10.5194/acp-8-1153-2008.

[21] G. C. Roberts, A. Nenes, *Aerosol Sci. Technol*. **2005**, *39*, 206, DOI: 10.1080/027868290913988.

[22] M. Paramonov, P. P. Aalto, A. Asmi, N. Prisle, V.-M. Kerminen, M. Kulmala, T. Petäjä, *Atmos. Chem. Phys*. **2013**, *13*, 10285, DOI: https://doi.org/10.5194/acp-13-10285-2013.

[23] M. D. Petters, S. M. Kreidenweis, *Atmos. Chem. Phys.* **2007**, *7*, 1961, DOI: 10.5194/acp-7-1961-2007.

[24] R. D. Cook, Y.-H. Lin, Z. Peng, E. Boone, R. K. Chu, J. E. Dukett, M. J. Gunsch, W. Zhang, N. Tolic, A. Laskin, K. A. Pratt, *Atmos. Chem. Phys*. **2017**, *17*, 15167, DOI: https://doi.org/10.5194/acp-17-15167-2017.

[25] S. E. Paulson, P. J. Gallimore, X. M. Kuang, J. R. Chen, M. Kalberer, D. H. Gonzalez, *Sci. Adv*. **2019**, *5*, eaav7689, DOI: 10.1126/sciadv.aav7689.

[26] J. Schmale, S. Henning, B. Henzing, H. Keskinen, K. Sellegri, J. Ovadnevaite, A. Bougiatioti, N. Kalivitis, I. Stavroulas, A. Jefferson, M. Park, P. Schlag, A. Kristensson, Y. Iwamoto, K. Pringle, C. Reddington, P. Aalto, M. Äijälä, U. Baltensperger, J. Bialek, W. Birmili, N. Bukowiecki, M. Ehn, A. M. Fjæraa, M. Fiebig, G. Frank, R. Fröhlich, A. Frumau, M. Furuya, E. Hammer, L. Heikkinen, E. Herrmann, R. Holzinger, H. Hyono, M. Kanakidou, A. Kiendler-Scharr, K. Kinouchi, G. Kos, M. Kulmala, N. Mihalopoulos, G. Motos, A. Nenes, C. O'Dowd, M. Paramonov, T. Petäjä, D. Picard, L. Poulain, A. S. H. Prévôt, J. Slowik, A. Sonntag, E. Swietlicki, B. Svenningsson, H. Tsurumaru, A. Wiedensohler, C. Wittbom, J. A. Ogren, A. Matsuki, S. S. Yum, C. L. Myhre, K. Carslaw, F. Stratmann, M. Gysel, *Sci. Data* **2017**, *4*, 170003, DOI: 10.1038/sdata.2017.3.

[27] M. Paramonov, V.-M. Kerminen, M. Gysel, P. P. Aalto, M. O. Andreae, E. Asmi, U. Baltensperger, A. Bougiatioti, D. Brus, G. P. Frank, N. Good, S. S. Gunthe, L. Hao, M. Irwin, A. Jaatinen, Z. Jurányi, S. M. King, A. Kortelainen,

A. Kristensson, H. Lihavainen, M. Kulmala, U. Lohmann, S. T. Martin, G. McFiggans, N. Mihalopoulos, A. Nenes, C. D. O'Dowd, J. Ovadnevaite, T. Petäjä, U. Pöschl, G. C. Roberts, D. Rose, B. Svenningsson, E. Swietlicki, E. Weingartner, J. Whitehead, A. Wiedensohler, C. Wittbom, B. Sierau, *Atmos. Chem. Phys*. **2015**, *15*, 12211, DOI: 10.5194/acp-15-12211-2015.

[28] E. R. Graber, Y. Rudich, *Atmos. Chem. Phys*. **2006**, *6*, 729, DOI: https://doi.org/10.5194/acp-6-729-2006.

[29] J. L. Axson, N. W. May, I. D. Colón-Bernal, K. A. Pratt, A. P. Ault, *Environ. Sci. Technol.* **2016**, *50*, 9835, DOI: 10.1021/acs.est.6b01661.

[30] X. Fan, J. Song, P. Peng, *Atmos. Environ*. **2012**, *60*, 366, DOI: 10.1016/j.atmosenv.2012.06.063.

[31] T. B. Kristensen, L. Du, Q. T. Nguyen, J. K. Nøjgaard, C. B. Koch, O. F. Nielsen, A. G. Hallar, D. H. Lowenthal, B. Nekat, D. van Pinxteren, H. Herrmann, M. Glasius, H. G. Kjaergaard, M. Bilde, *J. Atmos. Chem*. **2015**, *72*, 65, DOI: 10.1007/s10874-015-9302-8.